

Citation for published version:
Reynolds, T, Harris, R & Chang, W-S 2012, 'Dynamic stiffness and damping of dowel-type connections for timber structures under service conditions', Paper presented at World Conference of Timber Engineering 2012, Auckland, New Zealand, 16/07/12 - 19/07/12 pp. 566-573.

Publication date: 2012

Document Version Early version, also known as pre-print

Link to publication

# **University of Bath**

# **Alternative formats**

If you require this document in an alternative format, please contact: openaccess@bath.ac.uk

Copyright and moral rights for the publications made accessible in the public portal are retained by the authors and/or other copyright owners and it is a condition of accessing publications that users recognise and abide by the legal requirements associated with these rights.

**Take down policy**If you believe that this document breaches copyright please contact us providing details, and we will remove access to the work immediately and investigate your claim.

Download date: 12. Mar. 2023



# DYNAMIC STIFFNESS AND DAMPING OF DOWEL-TYPE CONNECTIONS FOR TIMBER STRUCTURES UNDER SERVICE CONDITIONS

Thomas Reynolds<sup>1</sup>, Richard Harris<sup>2</sup>, Wen-Shao Chang<sup>3</sup>

ABSTRACT: When a dowel-type joint is part of a vibrating system, the connecters exert cycles of load on the timber in embedment at various angles to the grain. Where timber is used in long, tall and light structures, the dynamic response to wind load and human-induced vibration can be critical and joints contribute significantly, in terms of damping and stiffness, to the way the structure as a whole behaves. An experimental study is presented here into the behaviour of timber subject to embedment perpendicular to the grain by a dowel-type connector. It examines the energy dissipation and dynamic stiffness in a single dowel embedding into a tight-fitting half-hole in a piece of Douglas Fir softwood. Its conclusions give an insight into the behaviour under dynamic service loads of this basic element of a dowel-type connection. This work contributes to a more thorough understanding of the damping and stiffness characteristics of timber, which can lead to more accurate estimation of the dynamic response of timber structures.

KEYWORDS: Dowel, Connection, Dynamics, Vibration, Embedment, Damping

## 1 INTRODUCTION

Dowel-type connections are widely used in timber structures, and play an important part in determining their stiffness and strength. Research into the seismic behaviour of timber structures has shown that connections contribute greatly to damping in the structure. Heiduschke [1, 2], for example, successfully used a hysteretic model of a connection to model the seismic response of a laminated timber frame structure. The work presented here investigates dynamic stiffness and damping under service loads, where there is no yield of the connector, and the tests address the interaction of a rigid dowel and the timber.

# 1.1 ENERGY DISSIPATION AND DAMPING

Much experimental research has been done into the dissipative post-yield behaviour of dowel-type connections. Awaludin [3] studied a bolted moment-resisting connection and Piazza et al. [4] investigated a connection with inclined screws. Both used hysteretic force-displacement diagrams to estimate the dynamic

stiffness and damping in the connection. Researchers have also put forward novel forms of connection which have good stiffness and dissipative behaviour under seismic loading: Awaludin tested a pre-tensioned bolted connection [5] and Leitjen et al. [6] a hollow tube connector. The methods used in the research presented here could enable development of connections with desirable pre-yield behaviour in service conditions.

Under seismic loading, the connectors behave plastically, dissipating energy. This mechanism of energy dissipation may not manifest itself under the smaller deformations associated with vibrations in service conditions, but other mechanisms, such as internal friction in the timber, friction along the dowel, as it is pulled through the hole and friction around the dowel, as it embeds into the timber, all have the potential to dissipate energy under small vibrations.

#### 1.2 DYNAMIC STIFFNESS

In the post-yield behaviour associated with seismic loading, researchers have also noted a change in stiffness in dowel-type connections. Awaludin et al. [5] note a reduction of stiffness with repeated cycles of load and Chui and Li [7] develop and test a model for a nailed connection incorporating a degradation in stiffness.

The prediction of the static stiffness and ultimate load capacity of dowel-type connections is normally based on tests on an individual dowel embedded into a timber piece. From the results of those tests, empirical rules have been generated for embedment strength and

<sup>&</sup>lt;sup>1</sup> Thomas Reynolds, PhD Student, BRE Centre for Innovative Construction Materials, University of Bath, Bath, BA2 7AY, UK. Email: t.p.s.reynolds@bath.ac.uk

<sup>&</sup>lt;sup>2</sup> Richard Harris, Professor of Timber Engineering, BRE Centre for Innovative Construction Materials, University of Bath, Bath, BA2 7AY, UK. Email: r.harris@bath.ac.uk

<sup>&</sup>lt;sup>3</sup> Wen-Shao Chang, Lecturer, BRE Centre for Innovative Construction Materials, University of Bath, Bath, BA2 7AY, UK. Email: wsc22@bath.ac.uk



stiffness which allow design of connections according to design codes.

This work aims to extend those test methods to assess the dynamic stiffness and damping characteristics of the connection under the pre-yield loads experienced by a joint in service conditions. This was done by measuring the secant stiffness and energy dissipated in a specimen under cyclic loading using force-displacement diagrams. Cycles of compressive load were applied to the dowel to approximate the forces it would experience as part of a vibrating structural system. The mean value and amplitude of the cyclic load was varied, to represent the range of dynamic loads experienced by structures in service conditions.

# 2 METHOD

The test method used here is an extension of a standard test for assessing the embedment strength and foundation modulus of a dowel. A sinusoidal variation of load is used to represent simple harmonic motion in a vibrating structure.

#### 2.1 STANDARD TEST METHODS

Test methods for assessing the stiffness and strength of dowel-type connections are defined by, amongst others, European Norm EN 383 [8] and the American Society for Testing and Methods ASTM 5764 [9]. The major difference between these methods is that the EN method uses a timber piece with a through hole, while the ASTM method uses a piece with a half hole in the surface. This means that using the ASTM method, the dowel can be held rigidly straight as it is loaded, while for the EN method, allowance must be made for the contribution of the deformation of the dowel to the deflection of the loading head. Santos et al. [10] compared the results of tests using the two methods, and found 'very close agreement' between the values of foundation modulus and embedment strength obtained by the ASTM and EN methods.

In choosing the test method for these dynamic tests, consideration must be given not just to the contribution of the dowel deformation to the stiffness of the specimen, but also to the energy dissipation that it exhibits, and while the European norm incorporates a correction for deformation of the dowel, it is considered that it would not be possible to use a reliable correction for the energy dissipated by the dowel deformation and the loading apparatus. The ASTM method provides the minimum energy dissipation in the loading apparatus, and so was chosen for these tests.

## 2.2 MATERIALS

The timber specimens were selected to be free from major defects. The timber was stored at a temperature of  $20\pm2^{\circ}\mathrm{C}$  and a relative humidity of  $65\pm5\%$  prior to testing. The change in moisture content was measured by monitoring the weight of one specimen, and the tests were carried out once the change of mass of that specimen was less than 0.1% per day. The change in weight of the specimen is shown in Figure 1.

The geometry of the specimen complies with the requirements of ASTM D5764. This standard only specifies minimum dimensions for the timber piece, and so the dimensions used, shown in Figure 3, were chosen so that they also comply with EN 383, to aid comparison with work done by other researchers.

The timber was weighed after drying and cutting into shape for testing, in order to determine its density. All the test pieces were weighed, giving an average density of 469kg/m<sup>3</sup>.

The moisture content of 7 of the test specimens was tested using the oven dry method according to BS EN 13183 [11]. The average moisture content of the specimens tested was 15.5%. On this basis, the dry density was estimated as 417kg/m<sup>3</sup>.

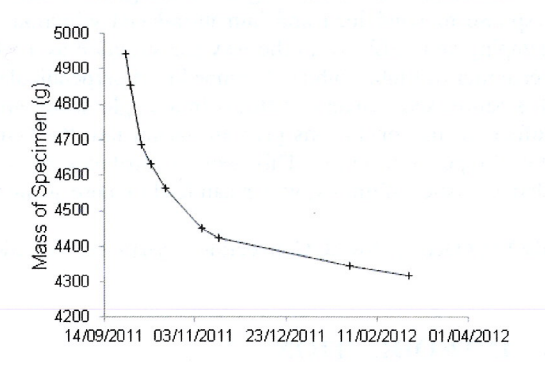


Figure 1: Drying of Douglas Fir

The same 20mm diameter plain high-tensile steel dowel, shown in Figure 2, was used for every test.

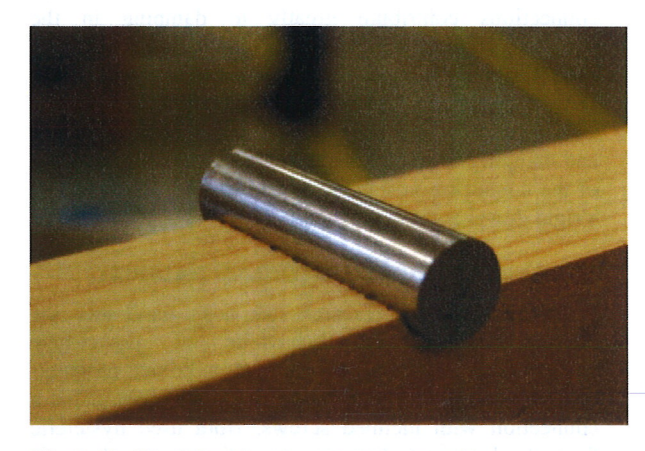


Figure 2: Steel dowel

#### 2.3 APPARATUS

The test setup for both the static and dynamic tests is shown schematically in Figure 3, and as a photograph in Figure 4. A servo hydraulic loading machine was used to apply load to a flat steel plate on top of the dowel. A linear variable differential transformer (LVDT) with a range of  $\pm 1 \, \mathrm{mm}$  was used to measure displacement, except when that range was exceeded, in which case the built-in-displacement transducer in the loading machine was used. This was the case only for the specimens loaded to 100% of the static yield load.

The servo hydraulic loading machine used was capable of applying loads up to 200kN. The gain for the built-in load cell could be adjusted, and for these tests was set for a range of  $\pm 20$ kN to ensure the best possible resolution of the load measurements.

In order to eliminate hysteresis from the displacement measurement, an LVDT was used which had no contact between its fixed and moving parts. This meant that there was no force transferred to the mounting of the LVDT. Any force in the mounting would have caused it to move, changing the measured displacement, and potentially introducing some hysteresis into the measurement.

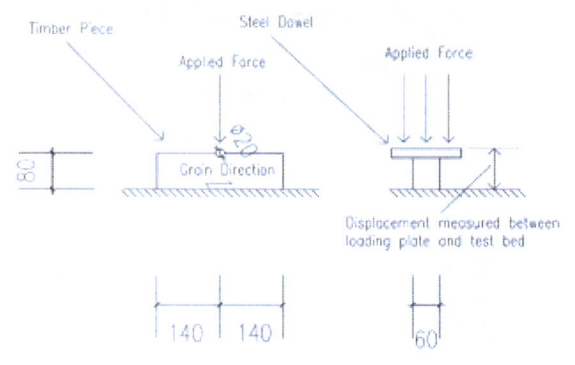


Figure 3: Schematic diagram of test setup (Dimensions in millimetres)

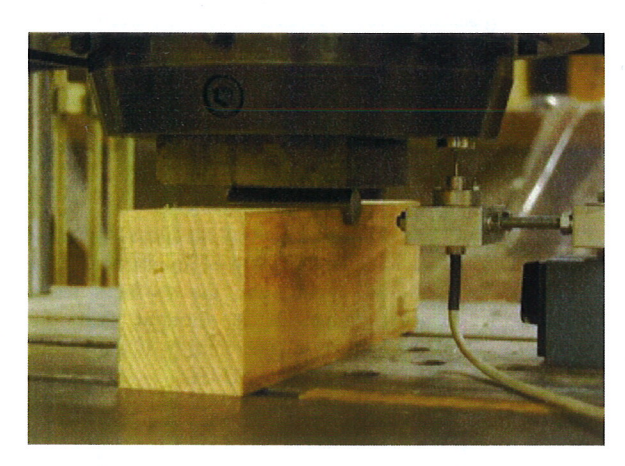


Figure 4: Test apparatus and sample

## 2.4 MICROSCOPY

Specimens were prepared for microscopy by cutting with a band saw vertically through the dowel hole. The pieces were then sanded with progressively finer abrasive paper until the trachieds of the timber were visible under an optical microscope. A microscope with magnification up to 500x was used.

# 2.5 LOADING

#### 2.5.1 Assessment of yield load

Eurocode 5 [12] predicts the embedment strength for a dowel loaded parallel to the grain based on the density of the timber parent material and the diameter of the dowel according to Equation (1) below:

$$f_{h,0,k} = 0.082(1 - 0.01d)\rho_k \tag{1}$$

where  $f_{h,0,k}$  = characteristic embedment strength parallel to the grain, d = dowel diameter,  $\rho_k$  = timber density. The embedment strength is then modified using Equation (2), based on that proposed by Hankinson [13], to give an embedment strength perpendicular to the grain.

$$f_{h,\alpha,k} = \frac{f_{h,0,k}}{k_{90} \sin^2 \alpha + \cos^2 \alpha} \tag{2}$$

where  $\alpha$  = the angle of embedment to the grain.  $k_{90}$  is a coefficient given by  $k_{90} = 1.35 + 0.015d$ .

The average dry density of the specimens, 406kg/m<sup>3</sup>, gave a characteristic embedment strength perpendicular to the grain of 19.4kN.

Quasi-static tests were carried out on two specimens according to ASTM D5764 to verify the calculated embedment strength. They resulted in a mean yield load of 17.5kN, and the force-displacement diagrams are shown in Figure 5. Since this was significantly lower than the characteristic value according to the Eurocode 5 calculation, this force was adopted as the yield load for definition of dynamic loads.

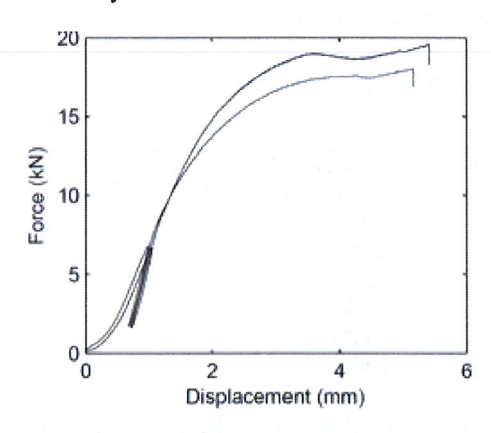


Figure 5: Force-displacement diagram from uasi-static tests

## 2.5.2 Definition of dynamic loads

Dynamic tests used a sinusoidal variation of force at a frequency of 1Hz. The amplitude of the sinusoidal applied load was defined by the R-ratio, which is given by the highest compressive load divided by the lowest compressive load:

$$R = \frac{P_{peak}}{P_{trough}} \tag{3}$$

Nominal R values of  $\infty$  and 1.2 were tested. R=1.2 representing small oscillation around a compressive average load and R= $\infty$  representing complete removal of the load in each cycle, since the lowest compressive load is zero.

BS EN 338 [14] states that, for softwoods, the characteristic value of modulus of elasticity should be taken as 67% of the mean value. It is assumed that this



relationship applies approximately for the yield strength. Eurocode 5 modifies the characteristic value of a resistance  $R_k$  according to Equation (4) to obtain the design value  $R_d$ .

$$R_d = \frac{k_{mod} R_k}{\gamma_m} \tag{4}$$

where the reduction factors  $k_{mod}$  and  $\gamma_m$  for instantaneous loading on solid timber are 1.3 and 1.1 respectively. The design value can therefore be taken to be 85% of the characteristic value, and 57% of the mean value.

On this basis, a connection with the mean value of resistance under its full design load would be at approximately 57% of its yield load. In service conditions, the applied loads are lower than the design loads, so the dynamic loads applied here were chosen as 30% and 50% of the mean yield load. The behaviour at 100% of the yield load was also investigated as an extreme case.

Each specimen was subjected to 1000 cycles of load at 1Hz. For two specimens, the effect of recovery was measured. 10% of the peak compressive load was applied for 30 minutes after the end of the test, before a further 400 cycles of load. The loads applied in the test are summarized in Table 1.

Table 1: Description of loading

Test	Peak Load P <sub>peak</sub>	R ratio
No.	(% of Static Yield)	$(P_{peak}/P_{trough})$
1	30%	1.2
2	30%	00
3	50%	1.2
4	50%	œ
5	100%	1.2
6	100%	œ

The non-linear behaviour of the dowel in embedment meant that the accuracy with which the servo hydraulic machine could apply the dynamic load was limited. It was found that, for the higher amplitude load cycles with  $R=\infty$ , the peak applied load exceeded the target value. For the cycles at 100% of the yield load, it was necessary to adjust the target values to ensure that the applied loads and displacements remained within safe limits.

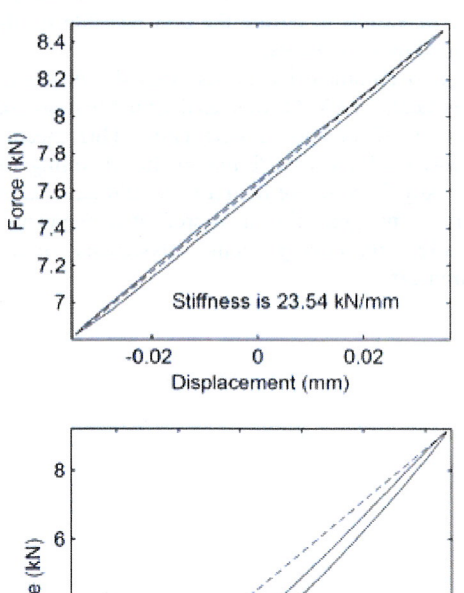
Displacement was measured using the LVDT for all tests except those with a peak load of 100% of the static yield load and  $R=\infty$ , for which the built-in displacement transducer in the loading machine was used.

# 3 RESULTS AND DISCUSSION

#### 3.1 DYNAMIC STIFFNESS

The secant stiffness was measured for each specimen under each cycle of load, as shown in Figure 6, by measuring the gradient between the point of maximum displacement and the point of minimum displacement. The measurement of secant stiffness in specimens loaded to 50% of the yield load with R=1.2 and  $R=\infty$  is shown.

It can be seen that the stiffness at  $R=\infty$  is reduced by the non-linear behaviour at low load.



Stiffness is 15.12 kN/mm

-0.2 -0.1 0 0.1 0.2 0.3

Displacement (mm)

**Figure 6:** Secant stiffness for a peak load of 50% of the static yield load, R=1.2 (top) and R=∞ (bottom)

Figure 7 shows the variation of secant stiffness through a typical test. There is an initial increase in stiffness over the first few hundred cycles, and the stiffness tends towards a constant value. It is thought that the densification of the timber in the vicinity of the dowel may cause this increase in secant stiffness.

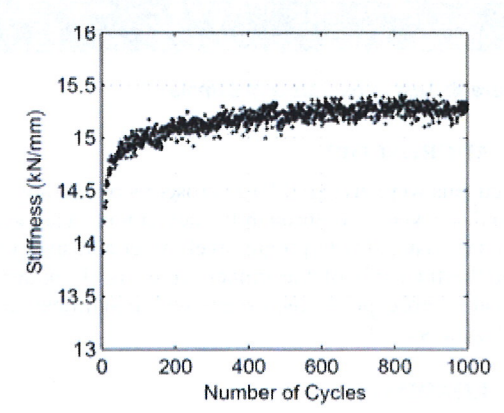


Figure 7: Variation of secant stiffness through the test for a peak load of 50% of the static yield load, R=∞

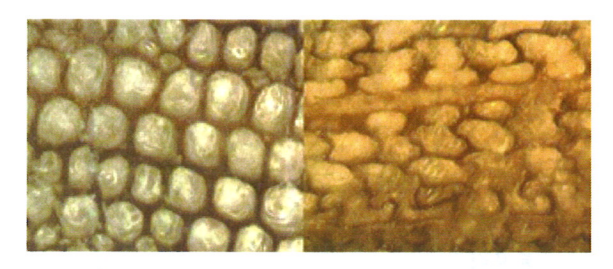


Figure 8: Undeformed earlywood cells and crushed cells in the vicinity of the dowel hole in a specimen loaded for 1000 cycles at a peak load of 50% of the static yield load, R=1.2. Optical magnification was 500x.

Figure 8 shows microscope images showing the permanent crushing of trachieds in the vicinity of the dowel. This densification could lead to an increase in the secant stiffness under dynamic loading.

It should be noted that the overall peak displacement of the dowel increases with each cycle of load, so the static stiffness of the joint would be considered to reduce throughout the test as the timber creeps. It is the secant stiffness, however, which determines the dynamic properties of the structure.

In order to estimate the constant value of stiffness in the latter part of the test, an average was taken of the secant stiffness in all the cycles after the 600th. This average value for each test is plotted against peak applied load in Figure 9.

There is a wide variation in secant stiffness between the tests. This variation does not appear to correlate with the density of the specimen as a whole. The three specimens with  $P_{peak} = 8.8kN$ , R=1.2, for example, show considerable scatter. The two specimens with secant stiffness greater then 35kN/mm had measured densities of 492 and 461kg/m<sup>3</sup>, while the one with secant stiffness below 25kN/mm had a measured density of 498kg/m<sup>3</sup>. In general, the stiffness in the tests at R=1.2 is higher than that in the tests at R=∞. This can be explained by

the effect of the non-linear behaviour at low loads, as shown in Figure 6 and described in Section 3.1.

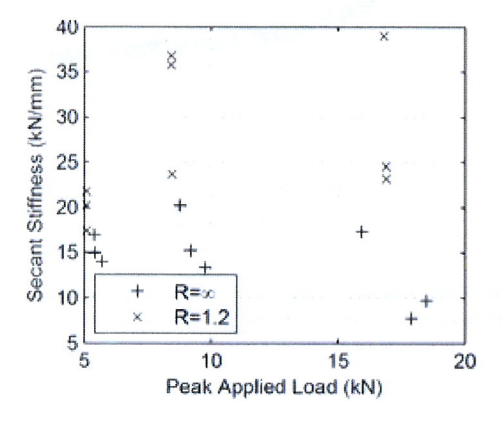


Figure 9: Variation of average secant stiffness with R ratio and peak applied load for all tests

## 3.2 DAMPING

The force-displacement diagrams for the early cycles exhibit significant creep in a single period, so that the hysteretic loop is not closed, but has the form shown in Figure 10.

The creep in each cycle contributes to damping, by increasing the area inside the hysteretic loop and therefore the energy dissipated. This effect is transient, however, and the hysteretic loops later in the test are closed, with the form shown in Figure 11.

It is observed that the transient damping due to creep is not the only source of energy dissipation in the system, and the closed loops later in the test still enclose an area. This energy dissipation may be a result of friction between the face of the dowel and the timber as the dowel embeds, and of internal friction in the microstructure of the timber.

Figure 12 plots the measured damping in each of the 1000 cycles in a typical test, expressed as the logarithmic decrement of structural damping. The damping is highest at the start, and tends towards a consistent value.

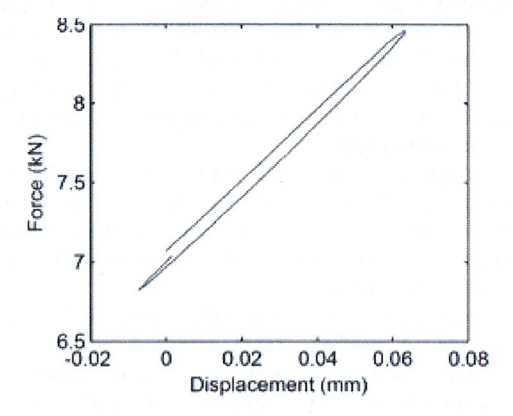


Figure 10: Force-displacement diagram for the 10<sup>th</sup> cycle, peak load of 50% static yield load R=1.2

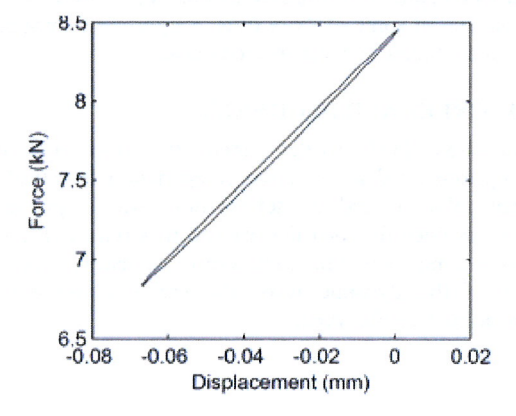


Figure 11: Force-displacement diagram for the 990th cycle, peak load of 50% static yield load R=1.2

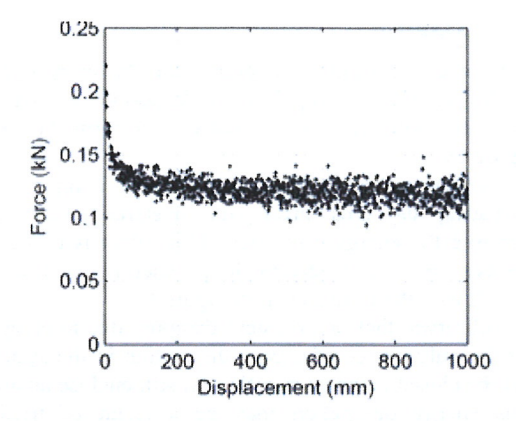


Figure 12: Variation of damping through the test for a peak load of 50% of the static yield load, R=1.2

In order to record the magnitude of the consistent damping towards the end of the test, the average damping measured in each cycle after the 600<sup>th</sup> was calculated. Figure 13 plots that average damping against the peak compressive force for all the tests. It can be seen that the consistent value of damping towards the end of the test is similar for each amplitude and peak load, with a slight increase in damping with magnitude of peak applied load.

The exception is for a peak load of 100% of the static yield load and  $R=\infty$ . Here gross deformation and fracture were observed in the timber during the test, which is thought to be responsible for the additional energy dissipation in that case.

In some specimens, particularly those with higher amplitude of loading, 1000 cycles appeared to be insufficient to reach a consistent value of damping, as shown in Figure 15. This can be explained by the fact that the tests with  $R=\infty$  impose the higher loads on the sample for only a short proportion of each cycle. The time under loading which the timber experiences is therefore less than in the equivalent test with R=1.2. The rate of creep is therefore lower in the tests with  $R=\infty$  and at the end of some of those tests, a significant amount of creep continues to occur in each cycle.

#### 3.3 CREEP AND RECOVERY

Dinwoodie [15] divides creep in timber into two components: a delayed elastic component, which leads to recoverable creep, a deformation which gradually reverses once the load that caused it is removed; and a plastic component which leads to irrecoverable creep. In two of the dynamic tests, the creep recovery after unloading was observed.

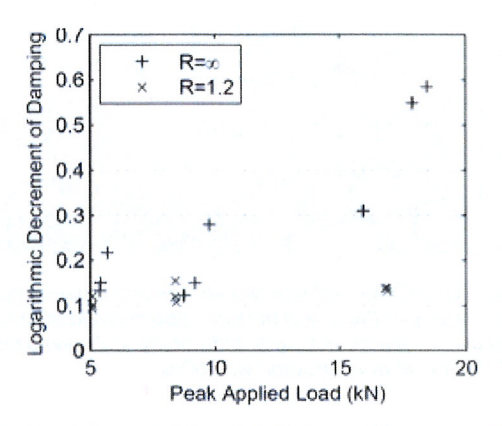
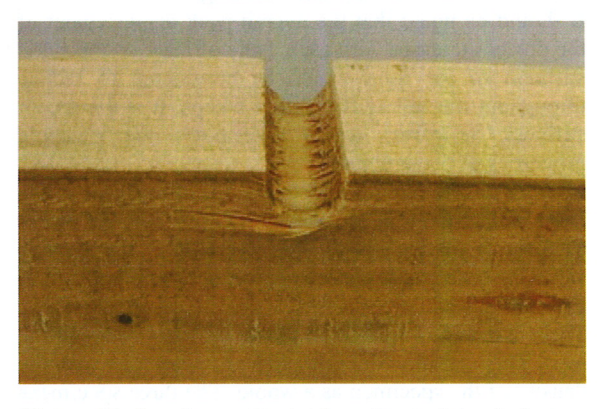


Figure 13: Variation of damping with R ratio and peak applied load for all tests



**Figure 14:** Specimen after testing at a peak load of 100% of the static yield load, R=∞.

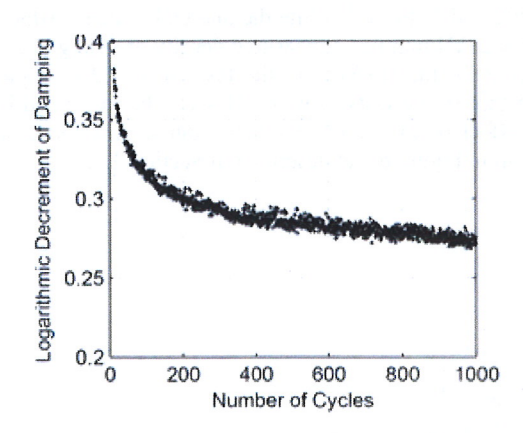
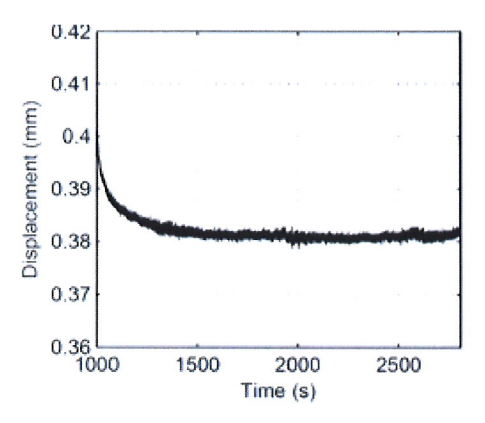


Figure 15: Variation of damping through the test for a peak load of 50% of the static yield load, R=10

After the 1000 cycles of load of the dynamic test, two specimens were subjected to a constant load of 10% of the peak applied load for 30 minutes. The recovery of the delayed elastic component of the displacement was monitored, and one set of results is shown in Figure 16. After the 30 minutes of recovery, 400 cycles of dynamic load were applied. Upon application of the cyclic load after recovery, it can be seen, in Figure 17, that the measured damping is initially higher than in the final cycles before recovery. This suggests that the creep that was recovered during the 30 minute period under 10% of the static yield load contributes to some transient damping in the second phase of cyclic loading. This behaviour could contribute to damping under short term dynamic loading.



**Figure 16:** Creep recovery under 10% of static yield load after 1000 cycles with peak value of 50% of static yield load, R=10

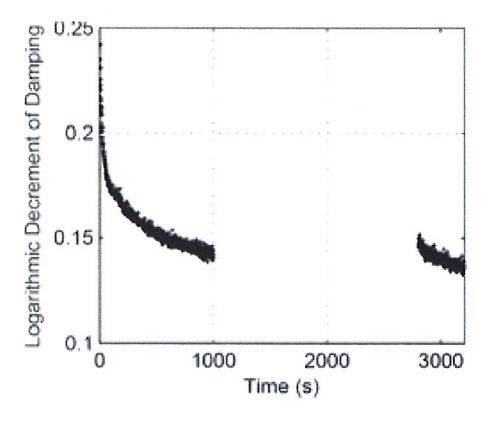


Figure 17: Variation of damping through the test for a peak load of 50% of the static yield load, R=10 with 30 minutes' recovery

# 4 CONCLUSION

The experimental work presented here showed that information about the dynamic behaviour of a dowel type connection can be obtained by a modified version of a standard test on a single dowel.

It has been shown that there is a large scatter in the secant stiffness of samples, which could lead to inaccuracy in prediction of natural frequencies of structural systems with dowel-type connections. Stiffness is generally higher for lower-amplitude dynamic loads, and the secant stiffness is observed to increase with repeated cycles of load.

The measured value of damping in each test appears to tend towards a consistent value over a number of cycles. This steady-state value of damping is similar for most of the tests, the exceptions being cases where the test was not long enough for the damping to reach a steady-state value, or where gross deformation and fracture occurred during the test.

Once the dowel is part of a joint between members, additional processes such as the deformation and pull-through of the dowel will contribute to the damping and stiffness of the connection. Further work is needed to assess the contribution of those processes to the dynamic stiffness and damping of the connection. This work provides the foundation, however, for analyzing the results of tests on whole connections.

The use of a half-hole specimen for these tests was practically useful to minimize dowel deformation and energy dissipation in the loading apparatus. Further analytical or practical work may be necessary to prove whether the energy dissipation and dynamic stiffness is significantly different in a full-hole specimen.

In the analysis of force-displacement diagrams for specimens under cyclic load to assess the variation of stiffness and damping, this work uses methods which have been successfully applied to vibration of timber structures under seismic loading. The results show the potential for such methods to be applied to vibrations under service loads, enabling more reliable design of timber structures for vibration in service conditions.

### **ACKNOWLEDGEMENT**

Thanks to Will Bazeley for his guidance in designing the test procedure, and to Atelier One for funding this research.

#### REFERENCES

- [1] Heiduschke, A. Analysis of wood-composite laminated frames under dynamic loads Analytical models and model validation. Part II: Frame model. *Progress in Structural Engineering and Materials*, 8(3): 111-119, 2006.
- [2] Heiduschke, A. Analysis of wood-composite laminated frames under dynamic loads Analytical models and model validation. Part I: Connection model. *Progress in Structural Engineering and Materials*, 8(3): 103-110, 2006.
- [3] Awaludin, A., Hayashikawa, T., Hirai, T. & Oikawa, A.: Dynamic Response of Moment Resisting Timber Joints. In., 5-7, Year.



- [4] Piazza, M., Polastri, A. & Tomasi, R. Ductility of timber joints under static and cyclic loads. *Proceedings of the ICE Structures and Buildings*, 164 (2): 79-90, 2011.
- [5] Awaludin, A., Hirai, T., Hayashikawa, T., Sasaki, Y. & Oikawa, A. Effects of pretension in bolts on hysteretic responses of moment-carrying timber joints. *Journal of Wood Science*, 54(2): 114-120, 2008
- [6] Leijten, A. J. M., Ruxton, S., Prion, H. & Lam, F. Reversed-Cyclic Behavior of a Novel Heavy Timber Tube Connection. *Journal of Structural Engineering*, 132(8): 1314-1319, 2006.
- [7] Chui, Y. H. & Li, Y. Modeling Timber Moment Connection under Reversed Cyclic Loading. *Journal of Structural Engineering*, 131(11): 1757-1763, 2005.
- [8] BS EN 383:2007, Timber structures. Test methods. Determination of embedment strength and foundation values for dowel type fasteners BSI, 2007.
- [9] D 5764, Standard Test Method for Evaluating Dowel-Bearing Strength of Wood and Wood-based Products (Reapproved 2002) Volume 4.10, ASTM, 1997.
- [10] Santos, C. L., De Jesus, A. M. P., Morais, J. J. L. & Lousada, J. L. P. C. A Comparison Between the EN 383 and ASTM D5764 Test Methods for Dowel-Bearing Strength Assessment of Wood: Experimental and Numerical Investigations. Strain, 46(2): 159-174, 2010.
- [11] BS EN 13183:2002, Moisture Content of a Piece of Sawn Timber Part 1 Determination by the Oven Dry Method, BSI, 2002.
- [12]BS EN 1995-1-1:2004+A1:2008, Eurocode 5 Design of timber structures Part 1-1: General — Common rules and rules for buildings, BSI, 2009.
- [13] Hankinson, R. Investigation of crushing strength of spruce at varying angles of grain. *Air service information circular*, 3(259), 1921.
- [14] BS EN 338, Structural timber. Strength classes BSI, 2009
- [15] Dinwoodie, J. M.: Timber its nature and behaviour. Spon London, 2000.